TRANSIENT INTERFERENCE SUPPRESSION VIA STRUCTURED LOW-RANK MATRIX DECOMPOSITION

Mao Li and Zishu He*

EE Department, Univ. of Electron. Sci. and Tech. of China, Chengdu, Sichuan 611731 China

ABSTRACT

Transient interference can dramatically degrade the performance of over-the-horizon radar (OTHR). A novel transient interference suppression method based on structured low-rank matrix decomposition is proposed in this paper. Unlike most of the traditional interference suppression methods which need three steps: detect interferences, excise corrupted data and reconstruct excised data, the proposed method formulates the interference suppression as a Hankel matrix decomposition problem and suppress the interference via a single process of optimization. In addition, the proposed algorithm can suppress not only the interferences including the weak and strong ones, but also the noise. Simulation and experimental results have demonstrated the effectiveness of the proposed method.

Index Terms— over-the-horizon radar (OTHR), transient interference suppression, low-rank matrix decomposition.

1. INTRODUCTION

High frequency (HF) over the horizon radar (OTHR) can detect the over-the-horizon targets via either the sky wave or the surface wave. This makes it useful primarily for the early warning radar role. Unfortunately, the OTHR signal is usually contaminated by transient interference, such as cosmic noises, lightnings, meteor echoes, man-made impulse bursts and other HF radiating sources, which can dramatically degrade the performance of OTHR system. Generally, since that the transient interferences possess some directional characteristics, they can be suppressed by the adaptive beamforming. However, it should be pointed out that adaptive beamforming cannot cancel the interferences received through the mainlobe of the antenna. In addition, most of the transient interferences in the HF band have powerful energy but with a short time duration and may still enter the radar receiver via the antenna sidelobes [1]. This has resulted in the development of slow time domain signal processing techniques for transient interference mitigation [1–6].

The basic ideas of traditional methods in [2–4] are quite similar. Firstly, interference occurrence position is detected by threshold method. Subsequently, the corrupted data are set to zero or excised from the received data and the missing data are reconstructed using autoregressive (AR) model. In [5], the missing data is reconstructs based on compressed sensing. In [1], a no-data interpolation method is proposed based on the adaptive time-frequency analysis technique, which detects the transient interference by the characteristics of short duration and strong energy. This time-frequency method can enhance the transient interference excision performance, particularly in cases where the durations of the interferences are relatively long compared to the coherent processing interval (CPI). However, it is usually more computationally expensive than the AR-based technique. For all the aforementioned algorithms, although the specific implementation details of the detection steps vary, all the detection methods of interferences are based on the simple property that the transient interference is short-lived on the time scale of the CPI but with powerful energy. Hence, in the cases where the interferences are weak, the traditional methods can not effectively detect and suppress them.

2. SIGNAL MODEL

The transient interference suppression step is generally performed after pulse compression and array beamforming, but prior to Doppler processing [1–6]. The received time-domain signal in a given azimuth-range cell within CPI can be modeled as [1]

$$r(m) = i(m) + n(m) + s(m),\ m = 1, \cdots, M \qquad (1)$$

where m denotes the slow time index, M is the number of pulses in CPI, $i(m)$ represents the transient interference, $n(m)$ denotes the noise, and $s(m)$ is the target-plus-clutter signal. According to the Bragg scattering hypothesis [7–9], the dominant sea clutter signal spectrum received by an H-F radar system can be characterized by a pair of spikes (or peaks) symmetrically placed about 0 Hz in the Doppler domain, known as the Bragg lines. The Doppler frequencies of the Bragg lines are given by $\pm f_B = \pm\sqrt{\frac{gf_c}{\pi c}}$, where f_c is the radar carrier frequency, g is the acceleration due to gravity, and c denotes the speed of light. However, in practice, the random and time-varying nature of the transmission medium, the ionosphere, may cause the Bragg lines to be extended in the Doppler domain. Hence, the sea clutter can be adequately

*Correspondence: limao164@163.com.

This work was supported by the National Nature Science Foundation of China under Grants 61032010 and 61102142.

modeled by [9, 10]

$$c(m) = a_1 e^{j(2\pi f_B mT + \varphi_1(m))} + a_2 e^{j(-2\pi f_B mT + \varphi_2(m))} \quad (2)$$

where a_1 and a_2 are the magnitudes of the positive and negative Bragg lines, $\varphi_1(m)$ and $\varphi_2(m)$ denote the phases of frequency modulations caused by the time-varying ionosphere, and T represents the pulse recurrence interval. Assume that the target is moving with constant radial velocity. Then, the target signal can be written as [11–13]

$$t(m) = be^{j2\pi f_d mT} \quad (3)$$

where b denotes the complex amplitude and f_d is the Doppler frequency. Combining (2) and (3), the target-plus-clutter echo in (1) can be rewritten as

$$\begin{aligned} s(m) =& c(m) + t(m) \\ =& a_1 e^{j(2\pi f_B mT + \varphi_1(m))} + a_2 e^{j(-2\pi f_B mT + \varphi_2(m))} \\ &+ be^{j(q_1 mT + \frac{1}{2} q_2 (mT)^2)}. \end{aligned} \quad (4)$$

3. TRANSIENT INTERFERENCE SUPPRESSION

3.1. Construct Low-rank and Sparsity Matrices

For the target-plus-clutter echo $s(m), m = 1, \cdots, M$, the Hankel matrix with m_1 rows and m_2 columns is constructed as

$$\mathcal{H}(s) = \begin{bmatrix} s(1) & s(2) & \cdots & s(m_2) \\ s(2) & s(3) & \cdots & s(m_2+1) \\ \vdots & \vdots & \ddots & \vdots \\ s(m_1) & s(m_1+1) & \cdots & s(M) \end{bmatrix} \quad (5)$$

where $M = m_1 + m_2 - 1$. It is shown in [9] and [14] that the sea clutter $c(m)$ may be considered as slow time-varying sinusoids in practice, i.e., the phases of frequency modulations $\varphi_1(m)$ and $\varphi_2(m)$ in (2) change significantly slow over the period of m_2. Then, according to [9], we have that the rank of $\mathcal{H}(s)$ will be close to 3. Generally, the number of pulses M, such as 256 or 512, is far greater than 3. Thus, we can always construct an approximate low-rank Hankel matrix $\mathcal{H}(s)$ using the sequence $s(m), m = 1, \cdots, M$, i.e., $\text{rank}(\mathcal{H}(s)) \ll \min(m_1, m_2)$.

In OTHR, the transient interferences are mainly due to lightning impulsive noises and meteor trail echoes [1, 15]. The durations of lightning and meteor are typically about 100-400ms [1, 2] and 0.5-1s, respectively. For the ship and aircraft detection tasks, the CPI is usually about 10-80s and 3-5s, respectively. Hence, the transient interference $i(m)$ in (1) always has a relatively short duration on the time scale of CPI, such that the interference Hankel matrix $\mathcal{H}(i)$, with the same structure as $\mathcal{H}(s)$ in (5), can be considered as a sparse matrix (a matrix populated primarily with zeros).

3.2. Suppression via Structured Matrix Decomposition

For notational simplicity, we use the notations of $\mathbf{R} = \mathcal{H}(r)$, $\mathbf{S} = \mathcal{H}(s)$, $\mathbf{I} = \mathcal{H}(i)$, and $\mathbf{N} = \mathcal{H}(n)$ to denote the complex Hankel matrices with respect to the received signal, target-plus-clutter signal, interferences, and noise sequences in (1), respectively. Then, the signal model in (1) can be expressed in the form of matrix as

$$\mathbf{R} = \mathbf{I} + \mathbf{N} + \mathbf{S} \quad (6)$$

where $\mathbf{I}$ are sparse Hankel matrix, $\mathbf{N}$ is noise matrix, and $\mathbf{S}$ is low-rank Hankel matrix. Matrix decomposition is a procedure for recovering an unknown matrix with low-rank or approximately low-rank constraint from a measurement matrix corrupted by errors or noise. Therefore, it is obvious that the suppression of the transient interference and the noise can be formulated as a matrix decomposition problem. In addition, the addition of structured prior information can improve the recovery performance of matrix. Considering that the low-rank matrix $\mathbf{S}$ has Hankel structure in (6), the transient interference suppression can be solved via the following optimization

$$\begin{aligned} &\min_{\mathbf{I},\mathbf{S},\mathbf{N}} \|\mathbf{S}\|_* + \lambda \|\mathbf{I}\|_1 \\ &\text{s.t. } \mathbf{R} = \mathbf{I} + \mathbf{N} + \mathbf{S}, \|\mathbf{N}\|_F \le \delta, \text{and } \mathbf{S} \in \mathcal{H} \end{aligned} \quad (7)$$

where $\|\cdot\|_*$ denotes the nuclear norm of a matrix (the sum of its singular values), $\|\cdot\|_1$ denotes the ℓ_1 norm of a matrix (the sum of the absolute values of matrix entries), $\|\mathbf{N}\|_F = \sqrt{\text{tr}(\mathbf{N}^H \mathbf{N})}$ is the Frobenius norm, the superscript $(\cdot)^H$ denotes conjugate transpose, $\text{tr}(\cdot)$ denotes the matrix trace, δ is the noise level, and λ is a trade-off constant for the sparse and the low-rank components. Mathematically, the Hankel constraint $\mathbf{S} \in \mathcal{H}$ in (7) can be expressed equivalently as

$$\mathbf{S} = \sum_{m=1}^{M} \alpha_m \mathbf{B}_m \quad (8)$$

where α_m is the complex weight coefficient and $\mathbf{B}_m \in \mathbb{R}^{m_1 \times m_2}$ is the basis matrix with the elements of the mth lower anti-diagonal elements equal to 1 and the others equal to zero. Then, the convex optimization problem in (7) can be rewritten as

$$\begin{aligned} &\min_{\mathbf{I},\mathbf{S},\mathbf{N}} \|\mathbf{S}\|_* + \lambda \|\mathbf{I}\|_1 \\ &\text{s.t. } \mathbf{R} = \mathbf{I} + \mathbf{N} + \mathbf{S}, \|\mathbf{N}\|_F \le \delta, \text{and } \mathbf{S} = \sum_{m=1}^{M} \alpha_m \mathbf{B}_m. \end{aligned} \quad (9)$$

It should be pointed out that the traditional matrix decomposition has been applied usually by considering real-valued data [16–19]. However, the received signals are complex-valued data in our signal model (1). It is shown in [20] that the problem of matrix decomposition for complex-valued data can be easily modified by arranging the real and imaginary parts of

the data in both real-valued matrices and applying matrix decomposition to these matrices. For the method in [20], the real and imaginary parts of the observed signal are decoupled, thus any prior phase information is not exploited. In order to exploit the phase information, we directly extend the real-valued matrix decomposition algorithm to complex-valued domain. We adopt the alternating direction method of multipliers (ADMM) [17, 21] method to solve the optimization problem (9). Define the augmented Lagrange function for the problem as

$$\ell(\mathbf{N},\mathbf{S},\boldsymbol{\alpha},\mathbf{I},\mathbf{Y}_1,\mathbf{Y}_2,\mu) = \|\mathbf{S}\|_* + \lambda\|\mathbf{I}\|_1 + \Re\langle\mathbf{Y}_1,\boldsymbol{\Delta}_1\rangle + \frac{\mu}{2}\|\boldsymbol{\Delta}_1\|_F^2 + \Re\langle\mathbf{Y}_2,\boldsymbol{\Delta}_2\rangle + \frac{\mu}{2}\|\boldsymbol{\Delta}_2\|_F^2 \tag{10}$$

where $\boldsymbol{\alpha} = [\alpha_1, \cdots, \alpha_M]^T$ is the complex weight coefficient vector, $\Re(\cdot)$ denotes the real part operator, $\boldsymbol{\Delta}_1 = \mathbf{R} - \mathbf{I} - \mathbf{N} - \mathbf{S} \in \mathbb{C}^{m_1\times m_2}$, $\boldsymbol{\Delta}_2 = \sum_{m=1}^{M}\alpha_m\mathbf{B}_m - \mathbf{S} \in \mathbb{C}^{m_1\times m_2}$, $\langle\mathbf{A},\mathbf{B}\rangle = \mathrm{tr}(\mathbf{A}^H\mathbf{B})$ denotes the matrix inner product, $\mu > 0$ is a penalty parameter, and the matrices $\mathbf{Y}_1, \mathbf{Y}_2 \in \mathbb{C}^{m_1\times m_2}$ are Lagrange multiplier matrices. Then, the solution can be approximated using an alternating strategy minimizing (10) with respect to each component separately [17, 21]

$$\begin{cases} \mathbf{N}_{k+1} = \arg\min\limits_{\|\mathbf{N}\|_F\le\delta} \ell(\mathbf{N},\mathbf{S}_k,\boldsymbol{\alpha}_k,\mathbf{I}_k,\mathbf{Y}_{1,k},\mathbf{Y}_{2,k},\mu_k) \\ \mathbf{S}_{k+1} = \arg\min\limits_{\mathbf{S}} \ell(\mathbf{N}_{k+1},\mathbf{S},\boldsymbol{\alpha}_k,\mathbf{I}_k,\mathbf{Y}_{1,k},\mathbf{Y}_{2,k},\mu_k) \\ \boldsymbol{\alpha}_{k+1} = \arg\min\limits_{\boldsymbol{\alpha}} \ell(\mathbf{N}_{k+1},\mathbf{S}_{k+1},\boldsymbol{\alpha},\mathbf{I}_k,\mathbf{Y}_{1,k},\mathbf{Y}_{2,k},\mu_k) \\ \mathbf{I}_{k+1} = \arg\min\limits_{\mathbf{I}} \ell(\mathbf{N}_{k+1},\mathbf{S}_{k+1},\boldsymbol{\alpha}_{k+1},\mathbf{I},\mathbf{Y}_{1,k},\mathbf{Y}_{2,k},\mu_k) \end{cases} \tag{11}$$

and

$$\begin{cases} \mathbf{Y}_{1,k+1} = \mathbf{Y}_{1,k} + \mu_k\boldsymbol{\Delta}_{1,k} \\ \mathbf{Y}_{2,k+1} = \mathbf{Y}_{2,k} + \mu_k\boldsymbol{\Delta}_{2,k} \\ \mu_{k+1} = \rho\mu_k \end{cases}. \tag{12}$$

Each of subproblems in (11) has a closed-form solution

$$\begin{cases} \mathbf{N}_{k+1} = \min(1,\delta\|\mathbf{Z}_k\|_F^{-1})\mathbf{Z}_k \\ \mathbf{S}_{k+1} = \mathbf{U}\mathcal{T}_{\frac{1}{2\mu_k}}(\boldsymbol{\Sigma})\mathbf{V}^H \\ \alpha_{m,k+1} = \|\mathbf{B}_m\|_1^{-1}\mathrm{tr}\{(\mathbf{S}_{k+1} - \frac{1}{\mu_k}\mathbf{Y}_{2,k})^T\mathbf{B}_m\} \\ \mathbf{I}_{k+1} = \mathcal{T}_{\lambda\mu_k^{-1}}(\mathbf{R} - \mathbf{N}_{k+1} - \mathbf{S}_{k+1} + \frac{1}{\mu_k}\mathbf{Y}_{1,k}) \end{cases} \tag{13}$$

where $\mathbf{Z}_k = \mathbf{R} - \mathbf{I}_k - \mathbf{S}_k + \mu_k^{-1}\mathbf{Y}_{1,k}$, $\mathbf{F}_k = 2^{-1}(\mathbf{R} - \mathbf{I}_k - \mathbf{N}_{k+1} + \sum_{m=1}^{M}\alpha_{m,k}\mathbf{B}_m + \mu_k^{-1}(\mathbf{Y}_{1,k} + \mathbf{Y}_{2,k}))$, and $\mathbf{F}_k = \mathbf{U}\boldsymbol{\Sigma}\mathbf{V}^H$ is the singular value decomposition (SVD) of $\mathbf{F}_k$. The soft thresholding operator $\mathcal{T}$ is defined as

$$\mathcal{T}_\varepsilon(x) = \begin{cases} (1 - \varepsilon\|x\|_1^{-1})x & \|x\|_1 > \varepsilon \\ 0 & \text{otherwise} \end{cases} \tag{14}$$

where x is a real or complex scalar and $\varepsilon > 0$. When $\mathcal{T}_\varepsilon(\cdot)$ is applied to matrix, it acts element-wise. In practice, the noise level δ is unknown. We estimate real noise level online by $\hat{\delta} = \|\mathbf{R} - \mathbf{S}_{k+1} - \mathbf{I}_{k+1}\|_F$ [22]. Since the estimation $\hat{\delta}$ is biased at the beginning iterations, we propose to start our algorithm with a relatively larger $\delta = \|\mathbf{R}\|_F$, and then reduce δ by a factor 0.2 until δ reach $\hat{\delta}$. In computation, the iteration can be terminated by

$$\max(\Lambda_{1,k},\Lambda_{2,k},\Lambda_{3,k},\Lambda_{4,k}) \le \eta \tag{15}$$

where $\eta > 0$ is a stopping tolerance for the relative change of two consecutive iterates, $\Lambda_{1,k} = \|\mathbf{S}_{k+1} - \mathbf{S}_k\|_F/\|\mathbf{S}_k\|_F$, $\Lambda_{2,k} = \|\boldsymbol{\alpha}_{k+1} - \boldsymbol{\alpha}_k\|_F/\|\boldsymbol{\alpha}_k\|_F$, $\Lambda_{3,k} = \|\mathbf{I}_{k+1} - \mathbf{I}_k\|_F/\|\mathbf{I}_k\|_F$, and $\Lambda_{4,k} = \|\mathbf{N}_{k+1} - \mathbf{N}_k\|_F/\|\mathbf{N}_k\|_F$. For completeness, the entire algorithm has been summarized as Algorithm 1.

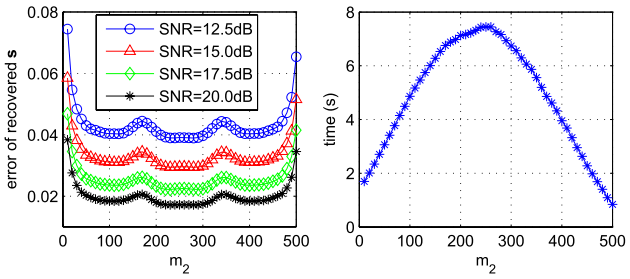

(a) Error (b) Running time

Fig. 1. Simulation results.

Algorithm 1. Solve problem (7) via ADMM.

Input:

Initial value: $\mathbf{I}_0 = \mathbf{0}$; $\mathbf{S}_0 = \mathbf{0}$; $\boldsymbol{\alpha}_0 = \mathbf{0}$; $\mathbf{Y}_{1,0} = \mathbf{0}$; $\mathbf{Y}_{2,0} = \mathbf{0}$; $k = 0$; $\eta = 10^{-5}$; $\mu_0 = 10^{-6}$; $\rho = 1.5$;

Received signal matrix $\mathbf{R}$ and $\lambda = (\max(m_1, m_2))^{-\frac{1}{2}}$.

1: **while** not converged **do**
2: Update $\mathbf{N}$, $\mathbf{S}$, $\boldsymbol{\alpha}$, and $\mathbf{I}$ by (13);
3: Update $\mathbf{Y}_1$, $\mathbf{Y}_2$, and $\boldsymbol{\mu}$ by (12);
4: Check the convergence conditions in (15);
5: **end while**

Output:

Recovered signal: $\hat{\mathbf{s}} = [\alpha_{1,k+1}, \cdots, \alpha_{M,k+1}]^T$.

4. SIMULATION AND EXPERIMENTAL RESULTS

1) Simulation results: The signal-to-clutter ratio (SCR) and signal-to-noise ratio (SNR) are defined as SCR $= 10\log\frac{\sum_{m=1}^{M}|t(m)|^2}{\sum_{m=1}^{M}|c(m)|^2}$ and SNR $= 10\log\frac{\sum_{m=1}^{M}|t(m)|^2}{\sigma^2}$, where σ^2 is the variance of noise. In simulation, we set SCR $= -40$dB and $M = 512$. Assume $a_1 = 1.5\times10^8$, $a_2 = 10^8$, $\varphi_1(m) = 0.425\cos(0.4\pi mT)$, $\varphi_2(m) = 0.775\cos(0.1\pi mT)$, and $f_d = -5$Hz.

In Fig.1(a), the error of recovered $\hat{\mathbf{s}}$ is plotted versus the number of matrix columns m_2, defined as

$$\text{error} = \frac{\|\hat{\mathbf{s}} - \mathbf{s}\|_F}{\|\mathbf{s}\|_F} \tag{16}$$

where $\mathbf{s} = [s(1), \cdots, s(M)]^T$ is the real target-plus-clutter echo. We see that the curves for smaller SNRs are higher than the ones for larger SNRs, which implies that larger SNRs lead to better recovering performance, as expected. It is also

observed that the proposed method has the best performance when $m_2 = M/2 = 256$. The reason may be the low-rank and sparsity constraints can be best fitted when $m_2 = M/2$. In Fig.1(b), however, we can find the running time for a MATLAB implementation is longest when $m_2 = M/2$. In simulation, we calculate the average running time via 50 implementations on a Dell desktop computer with a 3.1 GHz Intel Core 2 Duo processor and 2 GB of memory.

2) Experimental results: In this section, we will validate the transient interference suppression capability of the proposed method with the experimental data from a trial skywave OTHR. The CPI contains $M = 512$ pulses. We set $m_2 = M/2 = 256$.

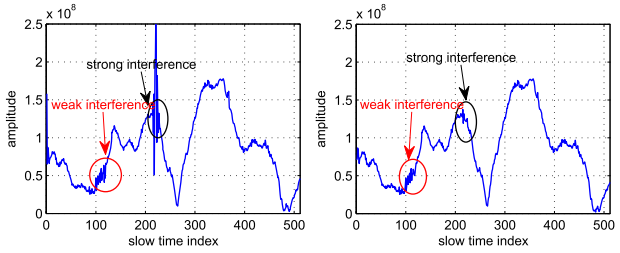

(a) Original signal (b) The time-frequency method

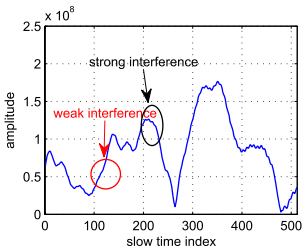

(c) The proposed method

Fig. 2. Amplitudes of signals.

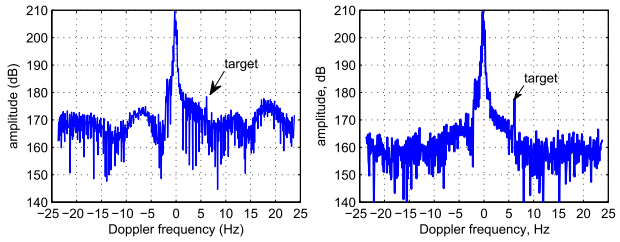

(a) Original signal (b) The time-frequency method

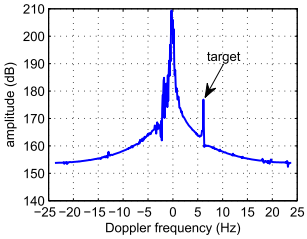

(c) The proposed method

Fig. 3. Doppler spectrums of signals.

For comparison, the adaptive time-frequency method in [1] is also applied to suppress the transient interference. Fig.2(a) shows the amplitude of a selected experimental data contaminated by the transient interference. We can clearly see that there are at least two transient interferences in the original signal, i.e., the weak and the strong interferences marked by the red and the black ellipses, respectively. The amplitude of strong interference is much higher than the underlying background level, but the weak interference is not obvious. Although the phenomenology and energy associated with both interferences maybe entirely different, it is obvious that the transient nature remains a common factor. Hence, both of interferences are sparse in the slow time domain. The amplitude of signal suppressed by the time-frequency method is presented in Fig.2(b). Comparing Fig.2(b) with Fig.2(a), it is obvious that the strong interference is almost completely excised, but the weak one is only removed slightly. In Fig.2(c), the corresponding amplitude of recovered data via the proposed method is plotted. It is seen that all the interferences, including the strong and weak ones, are suppressed, as expected, which justifies the proposed method can simultaneously mitigate weak and strong interferences. Fig.3(a) shows the Doppler spectrum of original signal. It can be seen that the background level is significantly high and has almost submerged the target peak. The spectrum of interference-removed signal obtained by the time-frequency method is shown in Fig.3(b). We can find that the background level is greatly reduced. Thanks to the reduction of the background level, the target peak becomes visible at about 6.1Hz. In Fig.3(c), the interference-removed spectrum via the proposed method is plotted. Comparing Fig.3(b) with Fig.3(c), it is obvious that the interference-removed signal via the proposed method has lower background noise level, making it possible for improving target detection performance in further signal processing. This shows that the proposed algorithm can not only suppress the interferences, including the weak and strong ones, but also the noise.

5. CONCLUSION

A unique method of the transient interference suppression is proposed in this paper based on the matrix decomposition. Unlike the traditional methods which employ energy feature of transient interference to detect the location of interference, the proposed method uses the sparsity of transient interference and the low-rank of target-plus-clutter signal to decompose the interference and target-plus-clutter components from the received echo. The detection and interpolation steps are not needed in the proposed method. Experimental examples show that the proposed method can not only effectively suppress the interferences, including the weak and strong ones, but also the noise. It should be pointed out that we also verified the performance and convergence of the proposed method by other simulation and experimental data. However, the results have not been included because of space limitations.

6. REFERENCES

[1] X. Guo, H. Sun, and T. S. Yeo, "Transient interference excision in over-the-horizon radar using adaptive time-frequency analysis," *IEEE Transactions on Geoscience and Remote Sensing*, vol. 43, no. 4, pp. 722–735, 2005.

[2] J. Barnum and E. E. Simpson, "Over-the-horizon radar sensitivity enhancement by impulsive noise excision," in *IEEE National Radar Conference*, pp. 252–256, 1997.

[3] X. Meng-Dao, B. Zheng, and Y. Qiang, "Transient interference excision in OTHR," *Acta Electronica Sinica*, vol. 6, pp. 823–826, 2002.

[4] M. Turley, "Impulsive noise rejection in HF radar using a linear prediction technique," in *Proceedings of the International Radar Conference*, pp. 358–362, 2003.

[5] Y. Quan, M. Xing, L. Zhang, and Z. Bao, "Transient interference excision and spectrum reconstruction for OTHR," *Electronics letters*, vol. 48, no. 1, pp. 42–44, 2012.

[6] X. Lu, J. Wang, A. Ponsford, and R. Kirlin, "Impulsive noise excision and performance analysis," in *IEEE Radar Conference*, pp. 1295–1300, May 2010.

[7] D. D. Crombie, "Doppler spectrum of sea echo at 13.56 Mc./s.," 1955.

[8] D. Barrick, "First-order theory and analysis of mf/hf/vhf scatter from the sea," *Antennas and Propagation, IEEE Transactions on*, vol. 20, no. 1, pp. 2–10, 1972.

[9] M. W. Poon, R. H. Khan, and S. Le-Ngoc, "A singular value decomposition (SVD) based method for suppressing ocean clutter in high frequency radar," *IEEE Transactions on Signal Processing*, vol. 41, no. 3, pp. 1421–1425, 1993.

[10] R. H. Khan, "Ocean-clutter model for high-frequency radar," *IEEE Journal of Oceanic Engineering*, vol. 16, no. 2, pp. 181–188, 1991.

[11] A. Yasotharan and T. Thayaparan, "Time-frequency method for detecting an accelerating target in sea clutter," *IEEE Transactions on Aerospace and Electronic Systems*, vol. 42, no. 4, pp. 1289–1310, 2006.

[12] J. Xu, X.-G. Xia, S.-B. Peng, J. Yu, Y.-N. Peng, and L.-C. Qian, "Radar maneuvering target motion estimation based on generalized radon-fourier transform," *IEEE Transactions on Signal Processing*, vol. 60, no. 12, pp. 6190–6201, 2012.

[13] G. Wang, X.-G. Xia, B. T. Root, V. C. Chen, Y. Zhang, and M. Amin, "Manoeuvring target detection in over-the-horizon radar using adaptive clutter rejection and adaptive chirplet transform," vol. 150, no. 4, pp. 292–298, 2003.

[14] K. Lu, X. Liu, and Y. Liu, "Ionospheric decontamination and sea clutter suppression for hf skywave radars," *IEEE Journal of Oceanic Engineering*, vol. 30, no. 2, pp. 455–462, 2005.

[15] S. Anderson, "Adaptive remote sensing with HF skywave radar," in *IEE Proceedings F*, vol. 139, pp. 182–192, 1992.

[16] E. J. Candès, X. Li, Y. Ma, and J. Wright, "Robust principal component analysis?," *Journal of the ACM (JACM)*, vol. 58, no. 3, pp. 11.1–11.37, 2011.

[17] Z. Lin, M. Chen, and Y. Ma, "The augmented lagrange multiplier method for exact recovery of corrupted low-rank matrices," *arXiv preprint arXiv:1009.5055*, 2010.

[18] G. Liu, Z. Lin, S. Yan, J. Sun, Y. Yu, and Y. Ma, "Robust recovery of subspace structures by low-rank representation," *IEEE Transactions on Pattern Analysis and Machine Intelligence*, vol. 35, no. 1, pp. 171–184, 2013.

[19] M. Tao and X. Yuan, "Recovering low-rank and sparse components of matrices from incomplete and noisy observations," *SIAM Journal on Optimization*, vol. 21, no. 1, pp. 57–81, 2011.

[20] H. Yan, R. Wang, F. Li, Y. Deng, and Y. Liu, "Ground moving target extraction in a multichannel wide-area surveillance SAR/GMTI system via the relaxed PCP," *IEEE Geoscience and Remote Sensing Letters*, vol. 10, no. 3, pp. 617–621, 2013.

[21] S. Boyd, N. Parikh, E. Chu, B. Peleato, and J. Eckstein, "Distributed optimization and statistical learning via the alternating direction method of multipliers," *Foundations and Trends® in Machine Learning*, vol. 3, no. 1, pp. 1–122, 2011.

[22] X. Zhou, C. Yang, and W. Yu, "Moving object detection by detecting contiguous outliers in the low-rank representation," *Pattern Analysis and Machine Intelligence, IEEE Transactions on*, vol. 35, pp. 597–610, March 2013.